Early detection of cardiac ischemia using a conductometric pCO_2 sensor: real-time drift correction and parameterization

2010 Physiol. Meas. 31 1241

(http://iopscience.iop.org/0967-3334/31/9/013)

IOP PUBLISHING PHYSIOLOGICAL MEASUREMENT

Physiol. Meas. **31** (2010) 1241–1255 doi:10.1088/0967-3334/31/9/013

Early detection of cardiac ischemia using a conductometric pCO_2 sensor: real-time drift correction and parameterization

Christian Tronstad[1], Soeren E Pischke[2,3], Lars Holhjem[2], Tor Inge Tønnessen[3,4], Ørjan G Martinsen[1,5] and Sverre Grimnes[1,5]

[1] Department of Clinical and Biomedical Engineering, Oslo University Hospital-Rikshospitalet, Norway
[2] The Interventional Centre, Oslo University Hospital-Rikshospitalet, Norway
[3] Clinic for Acute Medicine, Oslo University Hospital-Rikshospitalet, Norway
[4] Medical Faculty, University of Oslo, Norway
[5] Department of Physics, University of Oslo, Norway

Received 2 April 2010, accepted for publication 8 July 2010
Published 11 August 2010
Online at stacks.iop.org/PM/31/1241

Abstract

For detection of cardiac ischemia based on regional pCO_2 measurement, sensor drift becomes a problem when monitoring over several hours. A real-time drift correction algorithm was developed based on utilization of the time-derivative to distinguish between physiological responses and the drift, customized by measurements from a myocardial infarction porcine model (6 pigs, 23 sensors). IscAlert^{TM} conductometric pCO_2 sensors were placed in the myocardial regions supplied by the left anterior descending coronary artery (LAD) and the left circumflex artery (LCX) while the LAD artery was fully occluded for 1, 3, 5 and 15 min leading to ischemia in the LAD-dependent region. The measured pCO_2, the drift-corrected pCO_2 (ΔpCO_2) and its time-derivative ($TDpCO_2$) were compared with respect to detection ability. Baseline stability in the ΔpCO_2 led to earlier, more accurate detection. The $TDpCO_2$ featured the earliest sensitivity, but with a lower specificity. Combining ΔpCO_2 and $TDpCO_2$ enables increased accuracy. Suggestions are given for the utilization of the parameters for an automated early warning and alarming system. In conclusion, early detection of cardiac ischemia is feasible using the conductometric pCO_2 sensor together with parameterization methods.

Keywords: ischemia, pCO_2 sensor, biomedical signal processing, parameterization, drift

1. Introduction

1.1. pCO_2 as a clinical parameter

Monitoring of regional pCO_2 enables early detection of organ ischemia (Tønnessen and Kvarstein 1996, Tønnessen 1997, Kvarstein *et al* 2003, 2004). When the supply of O_2 to an organ is reduced below its O_2 demand, the cellular metabolism turns anaerobic. This change leads to a generation of protons by lactic acid and consumption of energy-rich phosphate compounds like ATP, which has to be buffered in order to reduce acidity. The buffering reaction of protons by bicarbonate yields CO_2 as a byproduct. In the case of arterial occlusion, the transport of excessive CO_2 from the affected region is impaired, leading to an increase in pCO_2 before anaerobic metabolism occurs. These processes contribute to the shape of the pCO_2 curve during an arterial occlusion. Using the generation rate of CO_2 together with the pCO_2 level may enable discrimination between these processes, utilizing the parameter $TDCO_2$ as introduced by Pischke *et al* (2010a, 2010b). Early detection of organ ischemia during hospitalization can ensure that intervention is performed before irreversible damage is caused. Cardiac ischemia (e.g. myocardial infarction) in the course of cardiac surgery and especially coronary artery bypass grafting (CABG) remains a major concern (Paparella *et al* 2007, Yau *et al* 2008) as it is a major determinant of post-operative mortality, morbidity and recurrence of angina pectoris symptoms (Force *et al* 1990, Steuer *et al* 2005). To date, reliable detection of perioperative myocardial infarction is insufficient as current clinical monitoring using ECG, blood pressure and observation of enzymatic blood parameters is confounded by the surgery, not specifically, or only taken once a day, respectively (Nass and Fleisher 2002).

1.2. The conductometric pCO_2 sensor

A biomedical pCO_2 sensor was presented by Mirtaheri *et al* (2004a). The sensor works by the principle of conductivity changes within an aqueous solution separated from the tissue by a gas-permeable membrane. The relation between the conductance of the solution volume and the pCO_2 at equilibrium is given by

$$G_{\text{total}} = \Psi \cdot (\sigma_0 + \left(\Lambda_{H^+}\vartheta_{H^+} + \Lambda_{HCO_3^-}\vartheta_{HCO_3^-}\right)(K \cdot K_H \cdot pCO_2)^{1/2}), \tag{1}$$

where Ψ (m) is a geometrical factor, σ_0 (S m^{-1}) is the conductivity at 0 kPa pCO_2, Λ (m^2(Ω mol)$^{-1}$) is the molar conductivity of ions, ϑ (unitless) is the activity of ions in the solution, K (mol l^{-1}) is the activity coefficient and K_H (mol (l kPa)$^{-1}$) is Henry's constant.

To enable compensation for the temperature dependence on the total conductance, a thermistor was embedded close to the electrodes within the sensor. This sensor was miniaturized into a biocompatible cylindrical design (1 mm diameter) for clinical use (Mirtaheri *et al* 2004b) and named the IscAlert^{TM} sensor. Sensors, connection units and calibration equipment used in this study were all produced and kindly provided by Alertis Medical ASA, Norway.

1.3. Sensor drift

Long-term instability is a well-known problem for the conductometric pCO_2 sensor (Varlan and Sansen 1997, Mirtaheri *et al* 2004a, 2004b) and the potentiometric pCO_2 (Zhao and Cai 1997) and pH (Gumbrell *et al* 1997, Mindt *et al* 1978, Drake and Treasure 1986) sensors. For the potentiometric sensors, a drift is significantly determined by the potential stability of the reference electrode (Guth *et al* 2009). For the conductometric sensor, there are several possible causes. As (1) shows, the total conductance is dependent on the sensor cell geometry.

For this sensor, the geometry depends on the tightness of the elastic membrane, which may change over time causing a drift as suggested by Mirtaheri *et al* (2004b). Another possibility is contamination of the aqueous solution from sensor parts or through ion leakage, which changes the total conductance by increasing the ion concentration or affecting the ion activity in (1). Electrically in series with the cell solution conductor, the electrode polarization impedance (EPI) is an important factor to the total conductance measurement and becomes increasingly dominant as the electrode area is reduced through sensor miniaturization. *In vitro* characterizations of electrodes of various sizes, materials and surface structures have revealed significant long-term changes in the EPI (Franks *et al* 2005, Kalvøy *et al* 2010), which makes this a likely cause of the conductometric drift. Increasing the excitation frequency for the measurement reduces the EPI contribution (Schwan 1992), but this is limited by the parasitic capacitance which becomes dominant at higher frequencies, especially for miniature sensor constructions. Until this problem is thoroughly investigated and the cause and remedy is found, other means of reducing drift such as real-time signal processing may offer an alternative.

For an automated detection and warning system for cardiac ischemia, a threshold pCO_2 detection limit cannot be used when a baseline wander is present. The aim of this study was to develop a real-time signal processing method for the earliest accurate detection of cardiac ischemia given the properties of the sensor, based on measurements from a porcine cardiac ischemia model.

2. Materials and methods

2.1. Animals and surgical procedure

The following protocol was approved by the Norwegian Animal Care and Use Committee and animals were handled according to the Revised Guide for the Care and Use of Laboratory Animals (NIH GUIDE, 1996).

Nine conventional landrace pigs (Sus scrofa), mean weight 59.2 kg (range 55–62 kg), male or female, were anesthetized, titrated to no reaction to skin incision during the whole experiment using pentobarbital (2–3 mg kg^{-1}), isoflurane (1, 5% flow) and morphine (0.5–1 mg kg^{-1} h^{-1}). Pigs were mechanically ventilated via a tracheostomy tube (Servo ventilator system 900 C, Siemens, Germany), and arterial pO_2 was kept above 11 kPa and arterial pCO_2 close to 5.5 kPa.

After sternotomy, the left anterior descending coronary artery (LAD) on the surface of the heart was identified and a flexible occluding string was placed distal to the second diagonal branch. Manual tightening of the occluding string leads to total occlusion of the LAD. This method has been shown to reliably reduce flow to $<10\%$ compared to the baseline (Nilsson *et al* 1995) and leads to loss of regional systolic contraction already after 1 min of occlusion (Espinoza *et al* 2010).

For gradual occlusion experiments, off-pump CABG from the left internal mammary artery to LAD was performed on three other pigs.

A sensor measuring tissue pO_2, pCO_2, pH and temperature (Neurotrend®, Codman, MA, USA) was inserted into the myocardium via a split needle in the LAD distribution area distal to the occlusion. Likewise, two or more IscAlert™ sensors were placed at the apex of the heart, in the area supplied by the LAD. After identification of the left circumflex artery (LCX), one sensor was placed in the area supported by blood from this artery. All sensors were consistently inserted approximately 5 mm subendocardially and at a distance of at least 5 mm from the designated coronary artery.

2.2. Experimental protocol

When stable measurements were achieved, the LAD was fully occluded for 1, 3, 5 and 15 min leading to ischemia in the LAD-dependent distribution area. For the gradual occlusions, blood flow in the bypass graft was measured with Doppler ultrasound flow probes (Medistim KirOp AS, Norway) and reduced to 75%, 50%, 25% and 0% in 18 min intervals using inflatable vascular occlusion devices (*In-Vivo* Metric, USA). Between ischemic events, at least 30 min of reperfusion with fully opened LAD was carried out. The animal was monitored for 2 h after the last occlusion and euthanized thereafter.

2.3. Sensors, calibration and pCO_2 prediction

As the conductance of the pCO_2 sensor also has a temperature dependence, calibration was performed according to the following model:

$$G_{\text{total}} = G_0 + k_{\text{pCO}_2} \cdot \text{pCO}_2 + k_T \cdot T, \tag{2}$$

where G_0 (S) is the sensor conductance at 0 kPa pCO_2 at 0 °C, k_{pCO_2} (μS kPa^{-1}) is a linear pCO_2 coefficient and k_T (μS °C^{-1}) is a linear temperature coefficient. With the sensor drift present, using the quadratic G versus pCO_2 relationship (1) for calibration and prediction would cause false changes in the pCO_2 versus G slope as G is reduced by the drift. A linear calibration ensures an equal slope over the whole range. Previous calibrations have shown that within the physiologically interesting pCO_2 range, the prediction accuracy is not reduced by this approximation. With large offsets often observed between calibration and usage, the linear relationship (2) was thus used in favor of the quadratic relationship (1).

Reference CO_2 solutions were produced by streaming of 5%, 10% and 15% CO_2 in N_2 gas standards (AGA AS) into sealed 100 ml glass bottles with 75 ml phosphate-buffered saline (Sigma-Aldrich Chemie). Five minutes of streaming with the respective CO_2 gases at 190 ml min^{-1} at room temperature (23 °C) produced CO_2 solutions at approximately 4, 7.5 and 11 kPa. The samples from the solutions were analyzed using an ABL700 blood-gas analyzer (Radiometer®) to obtain the 37 °C pCO_2 reference values. The temperature of the solutions was controlled using a Hart Scientific micro-bath (Fluke®). Sensor conductance was measured in each of the pCO_2 levels at three temperature levels of 30 °C, 34 °C and 38 °C giving a total of nine calibration points. Least-squares regression on these values was used to obtain the k_{pCO_2} and k_T, which would then be used for pCO_2 estimation by

$$\text{pCO}_2 = \frac{1}{k_{\text{pCO2}}}(G_{\text{total}} - G_0 - k_T \cdot T). \tag{3}$$

2.4. Data and acquisition

The sensor conductance was acquired using an IscAlert™ connection unit (CU) with 700 Hz ac conductance measurements using a 50 mV rms sine excitation. Acquisition was made using the IscAlert™ 2.0 software. The sampling rate was one sample every 5 s, which was the highest sampling rate available on the CU. The total length of the analyzed time series was from 2533 samples (3 h 31 min 5 s) at the minimum to 4426 samples (6 h 8 min 50 s) at the maximum. All the time series began at 30 min prior to the first occlusion, but due to differences in the length of the reperfusion phases given between occlusions, the total lengths varied.

Data from one pig were excluded due to ventricular fibrillation after 3 min of occlusion leading to death. The data from two other pigs were excluded due to IscAlert™ sensor malfunction with artifacts burying the signal of interest.

2.5. Drift correction and parameter extraction

The method of drift correction was based on utilization of the time derivative of the pCO_2 time series to distinguish between cases of sensor drift and true physiological pCO_2 changes in an ischemic heart. In the symbolic form, it is expressed as

$$\hat{p}(t) = \int^{t} \dot{p}(t) \cdot g(\dot{p}(t))\,\mathrm{d}t, \qquad g(\dot{p}(t)) = \begin{cases} 1, & \dot{p}(t) > D_{\max} \\ 1, & \dot{p}(t) < D_{\min} \\ 0, & \text{else}, \end{cases} \tag{4}$$

where $\dot{p}(t) = \frac{\mathrm{d}p(t)}{\mathrm{d}t}$.

$D_{\min}$ and $D_{\max}$ set the boundaries for the range of $\dot{p}(t)$ to be categorized as drift. The $\dot{p}(t)$ of the true responses are in general either higher than $D_{\max}$ during ischemia or lower than $D_{\min}$ during reperfusion. However, there can be some overlap between the $\dot{p}(t)$ of the drift and the last period of the return to baseline upon reperfusion due to its trend of exponential decay. This can cause a slight mismatch between the baselines before and after an occlusion and is solved by letting the $\hat{p}(t)$ return to baseline by exponential decay with a time constant matching the true decay when the $\hat{p}(t)$ is close to the defined baseline and the $\dot{p}(t)$ is within the drift range.

To determine the limits $D_{\min}$ and $D_{\max}$, the drifting of the sensors during the experiments was estimated by the difference in the temperature-corrected conductances at t_1 (30 min before the start of the first occlusion) and t_2 (35 min after the end of the last occlusion):

$$D = \frac{1}{t_2 - t_1}(G_{\text{total}}[t_2] - G_{\text{total}}[t_1] - k_T(T[t_2] - T[t_1])). \tag{5}$$

The median sensor drift was $-0.11\ \mu\text{S h}^{-1}$ with a maximum $0.0072\ \mu\text{S h}^{-1}$ and a minimum $-0.39\ \mu\text{S h}^{-1}$. The variation in the drift among the sensors based on the estimated pCO_2 was lower than for the temperature-corrected conductance by comparison of the inter-quartile range divided by the median. Thus, the time derivative of the estimated pCO_2 was used in favor of the conductance for the drift-correction algorithm. The median drift in pCO_2 was -0.38 kPa h^{-1} with a maximum of 0.025 kPa h^{-1} and a minimum of -1.37 kPa h^{-1}. This equals a minimum of -0.0019 kPa/5 s between two samples. $D_{\min}$ was set to -0.003 kPa/5 s and $D_{\max}$ to 0 kPa/5 s.

Before differentiation, the pCO_2 time series was low-pass filtered to avoid amplification of artifacts in the high-frequency range well above the true responses. The type of the filter was third-order zero-phase Butterworth with a cutoff frequency of 5 mHz.

The following real-time drift correction algorithm was developed and used, presented in the pseudo-code with the input x and output y:

Initialization:

$y[0] = \text{baseline}$

Continuous update:

$\mathrm{d}x[i] = x[i] - x[i-1]$
if $\mathrm{d}x[i] > \text{dmax}$ and $\mathrm{d}x[i-1] > 0$ and $\mathrm{d}x[i-2] > 0$
or
$\mathrm{d}x[i] < \text{dmin}$ and $\mathrm{d}x[i-1] < 0$ and $\mathrm{d}x[i-2] < 0$,
then$y[i] = y[i-1] + \mathrm{d}x[i]$,
else$\{y[i] = y[i-1]$; if $|y[i]| < 1$, then$y[i] = y[i] + k\,(\text{baseline} - y[i])\}$,

where $x[i]$ is the current pCO_2 measurement and $y[i]$ is the current drift-corrected pCO_2. The baseline variable can for instance be set to the initial value of x, but was set to zero in

our analysis because we were only interested in extracting the pCO_2 deviation from baseline (ΔpCO_2) for the ischemia detection. The coefficient k decides the speed of return to baseline when there are offsets below 1 kPa in the absolute value. The conditions on the two previous differentials to be larger than zero for the positive response case or less than zero for the negative response case were added to reduce noise and artifact susceptibility.

The algorithm was applied from 5 min into the time series (25 min prior to the first occlusion) to allow stabilization of the low-pass filter.

In addition to the ΔpCO_2 parameter, its time derivative ($TDpCO_2$), proportional to the generation rate of CO_2, was also calculated between each of the measurements:

$$TDpCO_2[i] = \frac{\Delta pCO_2[i] - \Delta pCO_2[i-1]}{T}, \tag{6}$$

where T is the sampling period.

For comparison between the ΔpCO_2 and the original pCO_2 measurements without drift correction, the original time series were baseline-adjusted to zero at the 5 min point and low-pass filtered using the same Butterworth filter as for the ΔpCO_2.

All the calculations were done using Matlab® v7.5.

2.6. Statistics

The time series of ΔpCO_2 and $TDpCO_2$ were split into four intervals, one for each of the occlusions including a range of 15 min prior to the occlusion and 25 min after the reperfusion. The maximum values within these intervals were used to determine the statistical significance between the measurements from the sensors placed in the distribution areas of LAD and LCX. The values could not be regarded as normally distributed based on the Lilliefors test; thus, the Wilcoxon rank-sum test was used for the determination of the p-values. The same values were used to determine the sensitivity and specificity of the ischemia detection ability during the different occlusions. Using the relation between the specificity and the detection limit, the detection limit for ΔpCO_2 was chosen as the value upon where 100% specificity was reached for all the occlusions (0.45 kPa). The $TDpCO_2$ detection limit was selected where $5/6 = 83\%$ specificity (explained in section 4) was obtained (0.092 kPa min^{-1}). Sensitivity and specificity was calculated for both parameters as

$$\begin{aligned} \text{Sensitivity} &= \frac{N_{\max(y_{\text{LAD}})\geqslant \text{lim}}}{N_{\max(y_{\text{LAD}})\geqslant \text{lim}} + N_{\max(y_{\text{LAD}})<\text{lim}}}, \\ \text{Specificity} &= \frac{N_{\max(\text{LCX})<\text{lim}}}{N_{\max(y_{\text{LCX}})<\text{lim}} + N_{\max(y_{\text{LCX}})\geqslant \text{lim}}}, \end{aligned} \tag{7}$$

where $\max(y)$ is the maximum ΔpCO_2 or $TDpCO_2$ in the LAD or LCX region within an occlusion interval, and lim is the selected detection limit for the parameter.

A separate analysis was done for the 15 min occlusion period, where the maximum ΔpCO_2 and $TDpCO_2$ at 1 min intervals each minute after the onset of the occlusion were extracted and used to calculate the sensitivity versus time. The same detection limits were used for the ΔpCO_2 and the $TDpCO_2$. The same statistics were also determined for the raw pCO_2 time series for comparison with the detection ability of the ΔpCO_2 using the same detection limit.

The tests were based on a total of 17 sensors from the LAD region and 6 control sensors in the LCX region.

To demonstrate that the presented drift correction method would also work for cases of gradual occlusion, especially with regard to preservation of the true responses, five time

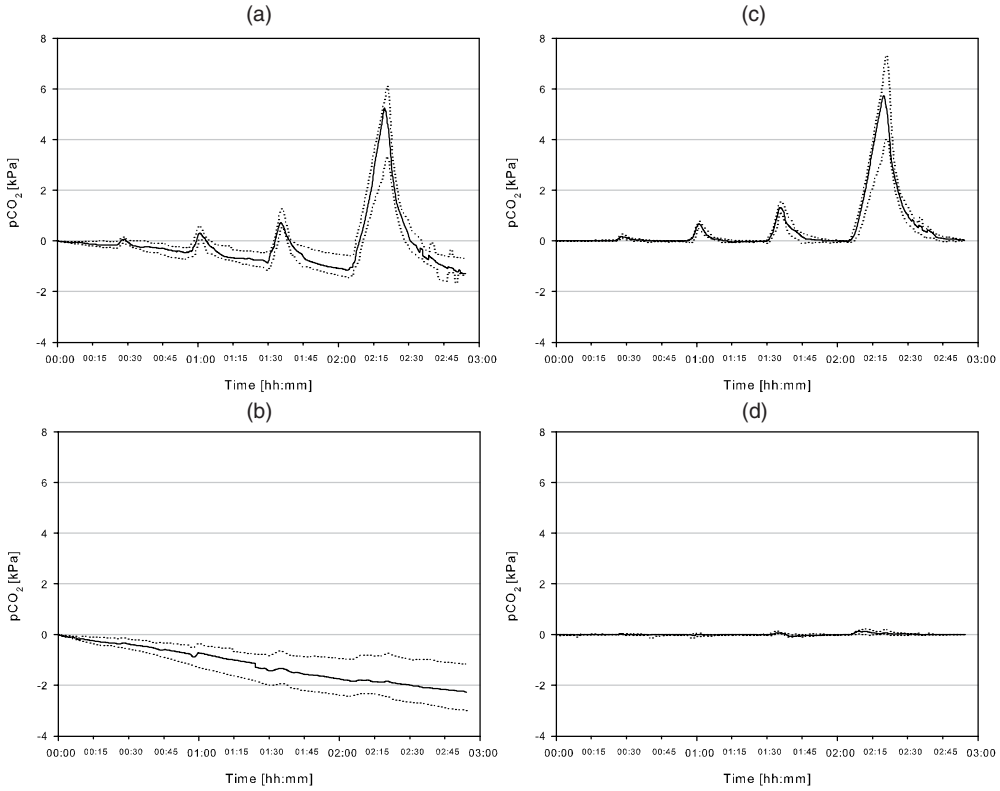

Figure 1. Medians (solid), 25% and 75% quartiles (dotted) for the original LAD ($N = 17$) (a), original LCX ($N = 6$) (b), drift-corrected LAD ($N = 17$) (c) and drift-corrected LCX ($N = 6$) (d). The original time series are also low-pass filtered using the same filter as for the drift correction and baseline adjusted to zero at the 5 min point for comparison. The time series in the plots were constructed from the occlusion intervals for synchronicity.

series from an ongoing study on gradual LAD occlusion were also included. The number of measurements from this protocol was not sufficient for a statistical analysis.

The statistics were also calculated using Matlab® v7.5.

3. Results

The algorithm corrected the drift for all the sensors while preserving the true physiological responses in the LAD-supplied region (figure 1). For the original data and at close to 3 h, the median baseline wandered to −1.3 kPa for the LAD sensors and −2.3 kPa for the LCX sensors, while the medians were 0.025 for the LAD and 0.0066 for the LCX when drift correction was applied. At the same time, the inter-quartile ranges of the LAD and LCX sensors were 0.77 and 1.85 kPa, respectively, while for the drift corrected time series they were 0.071 and 0.022 kPa. The true variations in the responses among the sensors during the occlusions were however preserved.

As shown in table 1, the 1 min occlusion led to a hypoxia (baseline was 4.95 kPa) within the LAD-supplied region, while the 3, 5 and 15 min occlusions caused anoxia. The drift-corrected pCO_2 (ΔpCO_2) had higher maximum values within the occlusion intervals than

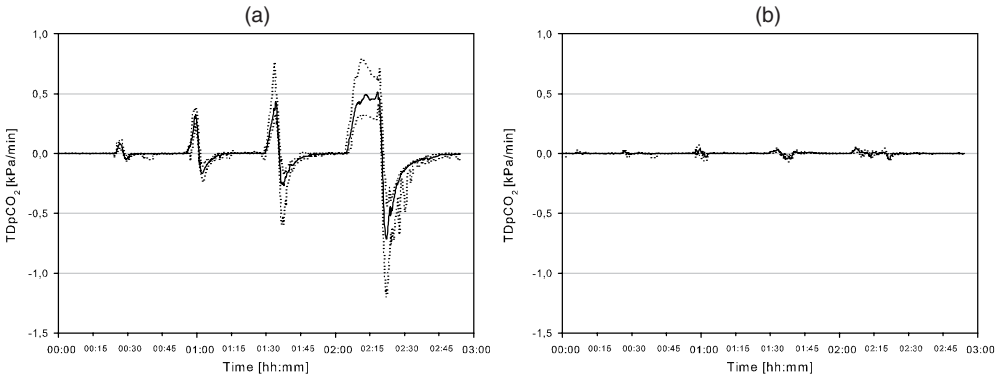

Figure 2. Medians (solid), 25% and 75% quartiles (dotted) for the TDpCO2 in LAD ($N = 17$) (a) and in LCX ($N = 6$) (b). The time series in the plots were constructed from the occlusion intervals for synchronicity.

Table 1. Statistics for the original pCO_2 (lowpass-filtered and baseline adjusted), the drift-corrected pCO_2 (ΔpCO_2) and the time-derivative of the pCO_2 ($TDpCO_2$) from the sensors placed in the LAD distribution area.

Occlusion duration (min)	Max pCO_2 (kPa)	Max ΔpCO_2 (kPa)	Max $TDpCO_2$ (kPa min^{-1})	Min pO_2 (kPa)	Sensitivity pCO_2	Sensitivity ΔpCO_2	Sensitivity $TDpCO_2$
1	0.10*	0.22**	0.12*	1.60	0.12	0.24	0.65
3	0.31**	0.69***	0.37***	0.00	0.35	0.82	1.00
5	0.78**	1.32***	0.45***	0.00	0.76	0.94	1.00
15	5.25***	5.74***	0.52***	0.00	1.00	1.00	1.00

The median of the maximum values within the different occlusion intervals among all the LAD sensors is presented along with the median of the minimum pO_2 within these intervals, measured by the Neurotrend sensor in the same region. The LAD max values are compared with the LCX max values (data not shown) within the same intervals using the Wilcoxon rank-sum test, $^{*}p < 0.05$, $^{**}p < 0.005$, $^{***}p < 0.0005$. The sensitivities are calculated with a detection limit of 0.45 kPa (100% specificity) for pCO_2 and 0.092 kPa min^{-1} (83% specificity) for the $TDpCO_2$. The statistics are based on 17 LAD sensors and 6 LCX sensors.

the uncorrected pCO_2 measurement, leading to a higher detection ability when using a pCO_2 threshold. The $TDpCO_2$ already reached a high value relative to the 15 min maximum after 3 min occlusion (table 1, figure 2) when anoxia occurred, leading to an earlier detection ability than the other parameters. Although all parameters yielded 100% sensitivity during the 15 min occlusion, figure 3 shows that this was first obtained at the 15th minute for the pCO_2, the 8th minute for the ΔpCO_2 and the 4th minute for the $TDpCO_2$, although with 83% specificity. The earliness of the detection ability was expectedly dependent on the detection limit, at the cost of the specificity as the limit is lowered toward zero. This relationship is shown in figure 4 with the time until 100% sensitivity was reached and the specificity is plotted against the detection limit. As presented in figure 5, combining the ΔpCO_2 and the $TDpCO_2$ can yield a 100% sensitivity with a 96% specificity for the 3, 5 and 15 min occlusions grouped together.

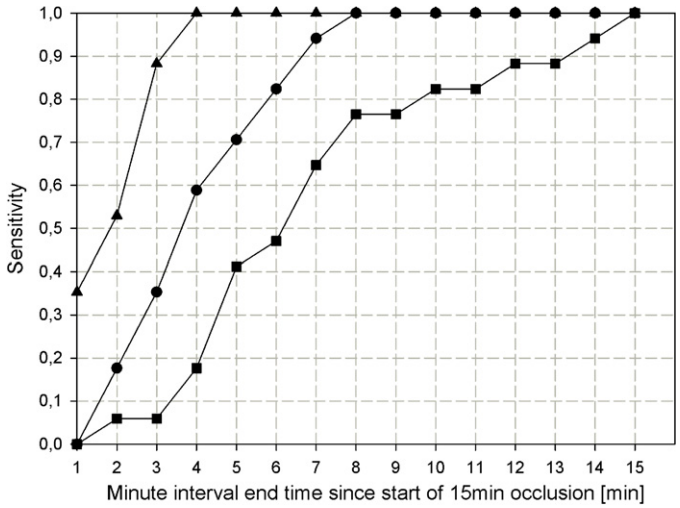

Figure 3. Sensitivities at each minute interval after the start of the 15 min occlusion for ΔpCO_2 (●) and the original pCO_2 (■) measurements with a detection limit of 0.45 kPa (100% specificity) and $TDpCO_2$ (▲) with a detection limit of 0.092 kPa min^{-1} (83% specificity).

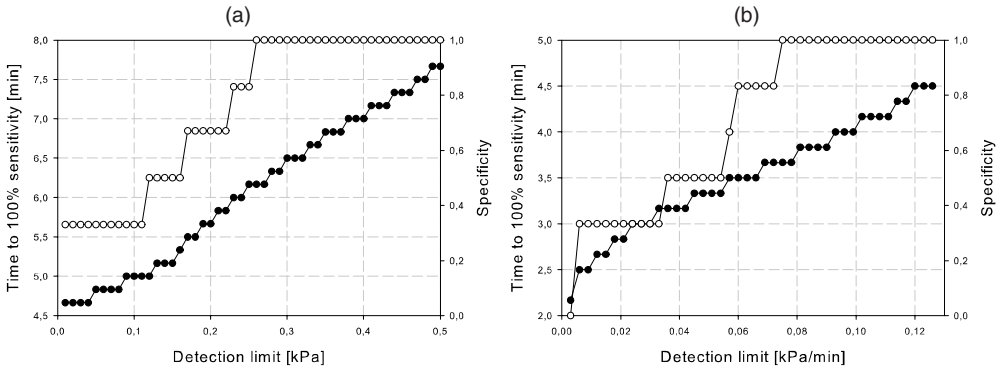

Figure 4. Time to 100% sensitivity after the start of occlusion (●) and specificity (○) versus detection limit for ΔpCO_2 (a) and $TDpCO_2$ (b) for the 15 min occlusion.

An example from one sensor during 15 min occlusion with a proposed utilization of the parameters for warning and alarm function is presented in figure 6. Figure 7 demonstrates that the method was also able to remove the drift without removing the true responses for cases of 25%, 50% and 75% LAD flow reduction.

4. Discussion

The drift correction causes stable values when there are slow negative changes in the measured pCO_2. The pCO_2 has been shown to return to the same baseline after successive occlusions in the same animal experiment, measured with the Neurotrend sensor (Pischke *et al* 2010a). Thus, we believe that the slow negative changes in the conductometrically measured pCO_2 are

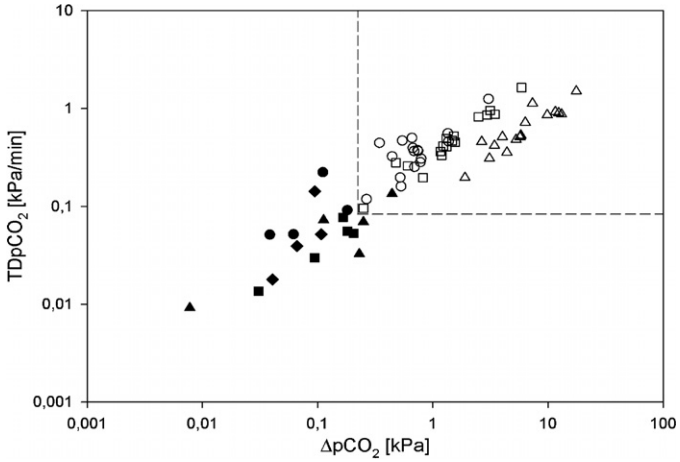

Figure 5. ΔpCO_2 versus $TDpCO_2$ plotted on logarithmic scales for the maximum values within the intervals of 3 min (○), 5 min (□) and 15 min (△) occlusion for the LAD-placed sensors and 1 min (♦), 3 min (●), 5 min (■) and 15 min (▲) for the LCX-placed sensors. 1 min LAD is not included as this occlusion did not yield anoxia. The dashed lines show the ability to separate the sensor responses from the ischemic area from those in the non-ischemic area using a combination of the ΔpCO_2 and $TDpCO_2$ as detection limits. In this case, the total sensitivity is 100% with a specificity of 96%.

exclusively due to drift and that the signal processing does not remove anything of physiological origin.

As shown in table 1, all the occlusion periods led to changes in pCO_2 measured by the sensors placed in the LAD region, which were significantly different ($p < 0.05$) from those placed in the control region LCX. Even though the 1 min occlusion did not lead to a real ischemia with pO_2 reaching zero, the small but significant pCO_2 increase may have been caused by the reduced flow inhibiting the CO_2 transport. The drift correction results in a better sensitivity for all the occlusions except for the 15 min event, where both sensitivities are 100%. However, the sensitivity versus time plot in figure 3 shows that within this interval, the event is detected earlier for the drift-corrected pCO_2 parameter.

The comparison between the original and the drift-corrected pCO_2 as presented in figure 1 shows the ability of the algorithm to extract only the physiologically interesting part of the time series. The evident drift in the negative direction in (a) and (b) eventually causes the offset to become large compared to the detection limit. To detect an ischemic event based on a pCO_2 level L, the measured pCO_2 would first have to increase above this offset and then reach L, resulting in an increased detection time as shown in figure 3 for the 15 min occlusion. A short occlusion at this time would perhaps not be detected at all. The offset increases linearly with time, as does the variance due to the differences in the drifting slopes.

The $TDpCO_2$ parameter is much less sensitive to drift. In addition, it brings additional information about the physiological processes by representing the CO_2 generation rate (Pischke *et al* 2010a, 2010b), which is not clearly seen by the shape of the pCO_2 curves. The transition between stasis and onset of metabolic ischemia could be distinguished by the $TDpCO_2$ parameter as the maximum CO_2 production will occur only during anaerobic metabolism when an excess of protons has to be buffered. $TDpCO_2$ will stay at its maximum until the substrate supply starts to wane. As the plot in figure 2(a) shows, the maximum $TDpCO_2$

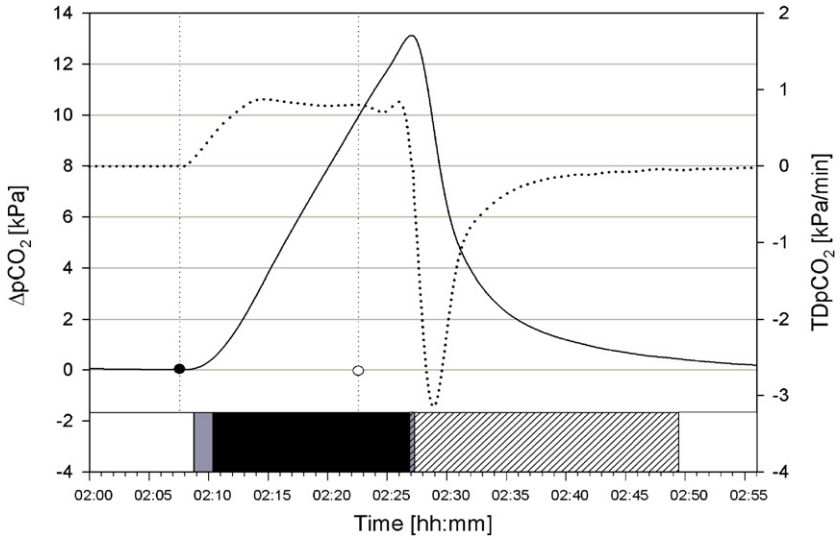

Figure 6. ΔpCO_2 (solid) and $TDpCO_2$ (dotted) before, during and after the 15 min occlusion ($\bullet$ = start, $\circ$ = end) for one of the sensors in the LAD region. The boxes in the lower end of the plot display different periods which are determined using the detection limits for the two parameters. Case 1 (white area) represents stable conditions when both parameters are below their limits. Case 2 (gray area) is a warning of a beginning ischemia when the $TDpCO_2$ is above its detection limit but ΔpCO_2 is still low. Case 3 (black area) shows the case of full ischemia when both parameters are above their detection limits. Case 4 (hatched gray area) indicates when the ΔpCO_2 is high but stable, with the $TDpCO_2$ between its detection limit and the negative drift limit. Case 5 (hatched white area) shows when the ΔpCO_2 is high, but returns toward the baseline with the $TDpCO_2$ below the negative drift limit.

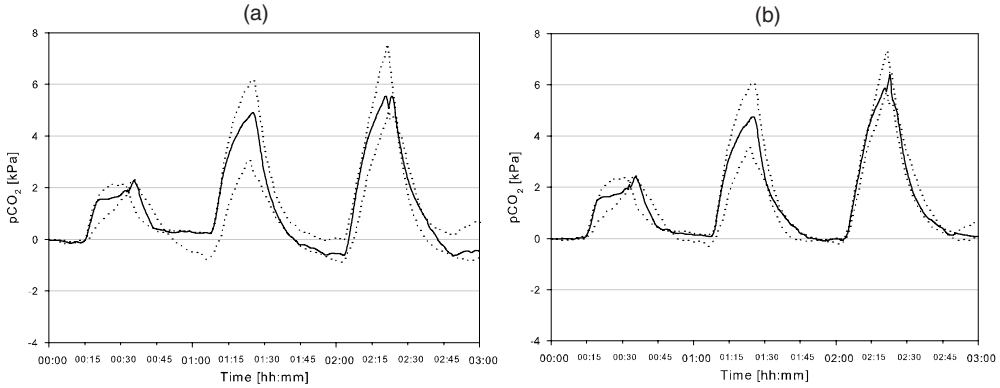

Figure 7. Median (solid), 25% and 75% quartiles (dotted) for the gradual occlusion time series from five sensors placed in the LAD-supplied region. Low-pass filtered and baseline-corrected original time series (a) and drift-corrected time series (b). From the left, flow reduction responses to 25%, 50% and 75% of the baseline LAD flow for 18 min.

within the 3, 5 and 15 min occlusion intervals are much higher than for the 1 min occlusion, where the pO_2 has not yet reached zero.

There is a trade-off between how early the ischemia can be detected and the specificity of the detection, depending on where the detection limit is set. As shown in figure 4(a),

a reduction in nearly 2 min can be gained by lowering the ΔpCO_2 detection limit from 0.45 kPa to a level which yields 66% specificity. For the $TDpCO_2$ in figure 4(b), a reduction in only about half a minute is gained by changing the detection limit similarly. We believe that a lowering of the detection limit below what gives 100% specificity is not worth the trade-off, as a high accuracy is desired in the clinical setting (Nass and Fleisher 2002). For the most accurate detection of ischemia, a combination of the ΔpCO_2 and the $TDpCO_2$ may be used as shown in figure 5 where the upper-right corner represents the cases where both the detection conditions for ΔpCO_2 and $TDpCO_2$ are met. This will avoid $TDpCO_2$ type 1 errors from transient artifacts and would avoid ΔpCO_2 type 1 errors if a positive drift or baseline offset should occur. However, in the clinical application it may be more important to avoid type 2 errors than type 1. A suggestion for the utilization of both the parameters is given in figure 6. During an occlusion, the changes are first detectable with the $TDpCO_2$ reaching a certain threshold (case 2). This case indicates that excessive CO_2 is being produced but the level is still close to the baseline, which could be implemented by a sort of warning. This warning would then turn to an alarm when the ΔpCO_2 crosses its detection limit (case 3). At some point the ΔpCO_2 may be high while the $TDpCO_2$ is close to zero (case 4). However, this has only been observed transiently in our measurements when the $TDpCO_2$ changes signs. A high ΔpCO_2 with a negative $TDpCO_2$ below D_{min} (case 5) indicates that the blood flow has returned, transporting the excessive CO_2 away from the tissue. This case eventually leads to a stable baseline where both parameters are close to zero (case 1). An additional case could be introduced by the condition of a stable, but high $TDpCO_2$ as an indicator of full ischemia.

It could be argued that the $TDpCO_2$ during the beginning of the occlusion may reflect the response characteristic of the sensor instead of the changes in tissue pCO_2. However, Mirtaheri *et al* 2004a reported the typical positive response time of the sensor to lie between 5 and 10 s while the $TDpCO_2$ increases for minutes during this phase (figure 6).

The source of the high-frequency artifacts was presumably the mechanical pressure oscillations in the beating heart acting on the sensor membrane causing geometrical changes to the volume of the sensor measurement cell, leading to oscillations in the conductance of the same frequency as the heart rate. With measurements sampled every 5 s, which was the highest available sampling rate using the IscAlert^{TM} connection unit, this artifact was greatly undersampled. This caused alias effects with a low-frequency content close to the true responses to appear on several occasions throughout the time series. Thus, the cutoff frequency had to be set as low as 5 mHz to remove as much alias as possible while keeping the true responses. A 5 mHz low-pass filter with a normal phase response would cause an undesired lag of 65 s. If the sample rate was at or above the Nyquist limit of the artifact, the phase lag would be no more than 2 s. Thus, a zero-phase filter was selected to more accurately determine the properties of the sensor regardless of the limits of the measurement electronics. With an excitation frequency of 700 Hz, oversampling the heart rate while keeping a good signal-to-noise ratio should not be an instrumentation problem. An anti-alias filter in the electronics could be an even simpler solution. Not all the alias could be removed from the time series by the low-pass filter without distorting the physiological signal. The remaining artifacts, although few, small in magnitude and transient, affected the $TDpCO_2$ parameter, especially in one control sensor. The detection limit of $5/6 = 83\%$ specificity was thus selected to reduce type 2 errors. Because this could be avoided with the appropriate instrumentation, we believe that the $TDpCO_2$ detection limit truly represents 100% specificity when considering the sensor properties regardless of the acquisition. With respect to detection of ischemia, the $TDpCO_2$ parameter itself is probably best suited for an early warning with a lesser confidence than the ΔpCO_2 or the combination of the two.

A similar method for real-time drift correction is the use of derivative-based operators in an IIR filter to remove low-frequency artifacts (Rangayyan 2002). This filter has the following time-domain form:

$$y[n] = \frac{1}{T}(x[n] - x[n-1]) + \alpha \cdot y[n-1]. \tag{8}$$

Although the filter has a sharp cutoff toward dc, it is not as sharp as the binary gain obtained using the case dependence in the presented filter algorithm. The pCO_2 curve contains important information when its derivative is very close to the limit of the drift. Thus, applying the filter (8) to our measurements would result in distortion of the signal shape during an ischemia, losing information about the course of the episode. This filter also has a nonlinear phase response and a tendency to introduce negative undershoot (Rangayyan 2002). We also need to be able to distinguish between the negative and positive drift because the sensor drift is in the negative direction and preservation of all the positive changes is needed. A conventional high-pass filter would always return the curves toward the baseline, but the presented algorithm allows this to occur only when below a limit of e.g. 1 kPa. A special case which may result in a type 2 error would occur if the pCO_2 curve was to flatten out completely below the 1 kPa limit with its time derivative within the defined drift range. However, we believe that this is unlikely to occur for a true ischemic event, as complete flattening has never been observed in any of our occlusions, not even above 1 kPa, and the $TDpCO_2$ will always be significantly higher than zero during anoxia. The negative drift would anyway drive this curve toward the baseline if it was not corrected. As shown in figure 7, the algorithm preserves the pCO_2 responses also for lesser degrees of blood flow reduction such as 75%, 50% or 25% of baseline flow.

For cases where the measurements contain single-point spike or step artifacts, including new limits in the algorithm for the highest allowed difference between the neighbor points will eliminate these. $g(\dot{p}(t))$ in (4) is then redefined to include the lowest allowed positive neighbor difference, A_+, and the lowest allowed negative neighbor difference A_- to be regarded as a spike:

$$g(\dot{p}(t)) = \begin{cases} 1, & \dot{p}(t) \in \{\langle D_{\max}, A_+ \rangle\} \\ 1, & \dot{p}(t) \in \{\langle D_{\min}, A_- \rangle\} \\ 0, & \text{else.} \end{cases} \tag{9}$$

However, when periodic high-frequency noise is superimposed as in the case of the measurements presented in this paper, a smoothing low-pass filter is necessary in order to preserve the more low-frequent true physiological measurement.

In summary, the following points should be met when applying this method for real-time automatic ischemia detection using the conductometric pCO_2 sensor:

- Common for invasive biosensors, there will be an initial stabilization phase after insertion. Applying the drift correction algorithm too early may include such transients in the ΔpCO_2, resulting in type 1 errors.
- The slope of the drift has to be separable from the slopes of the true responses. Although there is some overlap between the drift range of $\dot{p}(t)$ and the $\dot{p}(t)$ at the tail of the reperfusion phase for the sensor used in this study, this is the least critical part of the event. If the drift however would occur in the positive direction, with a large interindividual variation in slope, the early detection accuracy would be reduced.
- Artifacts in the high-frequency range should be reduced as much as possible in order to avoid $TDpCO_2$ type 1 errors, either by analog or digital filtering, but with a minimum of the phase lag.

In addition, rapid and large temperature fluctuations in the tissue may result in type 1 errors. The closed heart model used in this study ensured stable temperatures and consequently no temperature-induced artifacts in the measurements were observed.

In conclusion, the results show that a good accuracy for early real-time detection of cardiac ischemia is possible despite the inherent sensor drift when using the presented parameterization method.

Acknowledgment

Tronstad C and Pischke S E were financially supported by the Research Council of Norway.

References

Drake H F and Treasure T 1986 Continuous clinical monitoring with ion-selective electrodes: a feasible or desirable objective *Intensive Care Med.* **12** 104–7

Espinoza A, Halvorsen P S, Hoff L, Skulstad H, Fosse E, Ihlen H and Edvardsen T 2010 Detecting myocardial ischaemia using miniature ultrasonic transducers—a feasibility study in a porcine model *Eur. J. Cardiothorac. Surg.* **37** 119–26

Franks W, Schenker I, Schmutz P and Hierlemann A 2005 Impedance characterization and modeling of electrodes for biomedical applications *IEEE Trans. Biomed. Eng.* **52** 1295–302

Force T, Hibberd P, Weeks G, Kemper A J, Bloomfield P, Tow D, Josa M, Khuri S and Parisi A F 1990 Perioperative myocardial infarction after coronary artery bypass surgery. Clinical significance and approach to risk stratification *Circulation* **82** 903–12

Gumbrell G P, Peura R A, Kun S and Dunn R M 1997 Development of a minimally invasive microvascular ischemia monitor: drift reduction results *Proc. 10th Int. Conf. IEEE/EMBS (30 October–2 November)* **30** 25–7

Guth U, Vonau W and Zosel J 2009 Recent developments in electrochemical sensor application and technology—a review *Meas. Sci. Technol.* **20** 042002

Kalvøy H, Tronstad C, Nordbotten B, Martinsen Ø G and Grimnes S 2010 Electrical impedance of stainless steel needle electrodes *Ann. Biomed. Eng.* **38** 2371–82

Kvarstein G, Mirtaheri P and Tønnessen T I 2003 Detection of organ ischemia during hemorrhagic shock *Acta Anaesthesiol. Scand.* **47** 675–86

Kvarstein G, Mirtaheri P and Tønnessen T I 2004 Detection of ischemia by PCO_2 before ATP declines in skeletal muscle *Crit. Care Med.* **32** 232–7

Mindt W, Maurer H and Möller W 1978 Principle and characteristics of the ROCHE tissue pH electrode *Arch. Gynecol. Obstet.* **226** 9–16

Mirtaheri P, Grimnes S, Martinsen Ø G and Tønnessen T I 2004a A new biomedical sensor for measuring PCO_2 *Physiol. Meas.* **25** 421–36

Mirtaheri P, Omtveit T, Klotzbuecher T, Grimnes S, Martinsen Ø G and Tønnessen T I 2004b Miniaturization of a biomedical gas sensor *Physiol. Meas.* **25** 1511–22

Nass C and Fleisher L A 2002 Diagnosing perioperative myocardial infarction in cardiothoracic and vascular surgery *Sem Cardiothorac. Vasc. Anesth.* **6** 219–27

Nilsson S., Wikstrom G, Ericsson A., Wikstrom M., Waldenstrom A and Hemmingsson A 1995 MR imaging of gadolinium-DTPA-BMA-enhanced reperfused and nonreperfused porcine myocardial infarction *Acta Radiol.* **36** 633–40

Paparella D, Cappabianca G, Malvindi P, Paramythiotis A, Galeone A, Veneziani N, Fondacone C, Tupputi L and Schinosa L 2007 Myocardial injury after off-pump coronary artery bypass grafting operation *Eur. J. Cardiothorac. Surg.* **32** 481–7

Pischke S E, Tronstad C, Holhjem L and Tønnessen T I 2010a Real-time measurement of myocardial CO_2 tension and CO_2 generation rate reliably detects intermittent myocardial ischemia in a porcine model *Circulation* submitted

Pischke S E, Tronstad C and Tønnessen T I 2010b Peri- and postoperative real-time measurement of myocardial CO_2 tension and CO_2 generation rate as a promising clinical tool for detection of cardiac ischemia *39th Critical Care Congress of the Society-of-Critical-Care-Medicine (Miami, FL, 09–13 January 2010) Crit. Care Med.* **37** A87

Rangayyan R M 2002 *Biomedical Signal Analysis (IEEE Press Series in Biomedical Engineering)* (Piscataway, NJ: IEEE)

Schwan H P 1992 Linear and nonlinear electrode polarization and biological materials *Ann. Biomed. Eng.* **20** 269–88

Steuer J, Granath F, de Faire U, Ekbom A and Stahle E 2005 Increased risk of heart failure as a consequence of perioperative myocardial injury after coronary artery bypass grafting *Heart* **91** 754–8

Tønnessen T I 1997 Biological basis for PCO_2 as a detector for ischemia (review) *Acta Anaesthesiol. Scand.* **41** 659–69

Tønnessen T I and Kvarstein G 1996 PCO_2 electrodes at the surface of the kidney detect ischemia *Acta Anaesthesiol. Scand.* **40** 510–9

Varlan A R and Sansen W 1997 Micromachined conductimetric $p(CO_2)$ sensor *Sensors Actuators* B **55** 309–15

Yau J M *et al* 2008 Impact of perioperative myocardial infarction on angiographic and clinical outcomes following coronary artery bypass grafting (from PRoject of *Ex-vivo* Vein graft ENgineering via Transfection [PREVENT] IV) *Am. J. Cardiol.* **102** 546–51

Zhao P and Cai W J 1997 An improved potentiometric pCO_2 microelectrode *Anal. Chem.* **69** 5052–8